Visual function resists early neurodegeneration in the visual system in primary progressive multiple sclerosis

Sina Rosenkranz, Lilija Gutmann, Arzu Ceylan Has Silemek, Michael Dorr, Vivien Häußler, Margareta Lüpke, Andrea Mönch, Stefanie Reinhardt, Jens Kuhle, Penelope Tilsley, et al.

Visual function resists early neurodegeneration in the visual system in primary progressive multiple sclerosis

Sina C. Rosenkranz[1†], Lilija Gutmann[1†], Arzu Ceylan Has Silemek[1], Michael Dorr[2], Vivien Häußler[1], Margareta Lüpke[1], Andrea Mönch[1], Stefanie Reinhardt[1], Jens Kuhle[3], Penelope Tilsley[4,5], Christoph Heesen[1], Manuel A. Friese[1], Alexander U. Brandt[6,7], Friedemann Paul[6], Hanna Zimmermann[6], Jan-Patrick Stellmann[1,4,5]

[†]These authors contributed equally to this work.

1 Institut für Neuroimmunologie und Multiple Sklerose (INIMS), Universitätsklinikum Hamburg-Eppendorf (UKE), Hamburg, Germany
2 Adaptive Sensory Technology, Lübeck, Germany
3 Clinical Trial Unit, Department of Clinical Research, University Hospital Basel and University of Basel, Basel, Switzerland
4 APHM, Hopital de la Timone, CEMEREM, Marseille, France
5 Aix Marseille Univ, CNRS, CRMBM, Marseille, France
6 Experimental and Clinical Research Center, Max Delbrück Center for Molecular Medicine and Charité - Universitätsmedizin Berlin, Corporate Member of Freie Universität Berlin and Humboldt-Universität zu Berlin, Berlin, Germany
7 Department of Neurology, University of California Irvine, California, US

ABSTRACT

Background: Neurodegeneration in multiple sclerosis (MS) affects the visual system but dynamics and pathomechanisms over several years especially in primary progressive MS (PPMS) are not fully understood.

Methods: We assessed longitudinal changes in visual function, retinal neurodegeneration using optical coherence tomography, magnetic resonance imaging and serum NfL (sNfL) levels in a prospective PPMS cohort and matched healthy controls. We investigated the changes over time, correlations between outcomes and with loss of visual function.

Results: We followed 81 PPMS patients (mean disease duration 5.9 years) over 2.7 years on average. Retinal nerve fiber layer thickness (RNFL 90.1 vs. 97.8µm; p<0.001) was reduced in comparison to controls. Visual functioning quantified by the area under the log contrast sensitivity function (AULCSF) remained stable over a continuous loss of RNFL (0.46 µm/year, *95%CI: 0.10-0.82*; *p*=0.015) up until a mean turning point of 91µm, from which, the AULCSF deteriorated. Inter-eye RNFL asymmetry above 6 µm, suggestive of subclinical optic neuritis occurred in 15 patients and was related to lower AULCSF but occurred also in 5 out of 44 controls. Patients with an AULCSF progression had a faster increase in EDSS (*beta*=0.17/y, *p*=0.043)). sNfL levels were elevated in patients (12.2pg/ml vs. 8.0pg/ml, p<0·001), remained stable during follow-up (beta=–0·14 pg/ml/y, p=0·291) and were not associated with other outcomes.

Conclusion: Whereas neurodegeneration in the anterior visual system is already present at onset, visual function is not impaired until a certain turning point. sNfL was not correlated with structural or functional impairment in the visual system.

INTRODUCTION

Accumulation of disability in Multiple Sclerosis (MS) is driven by chronic inflammation leading to gradual neurodegeneration. The latter is considered a hallmark of progressive MS, being especially pertinent in primary progressive MS (PPMS).[1] Understanding and counteracting neurodegenerative processes are major unmet needs for all MS subtypes and studies in PPMS may help to mechanistically understand them. However, it is still challenging to detect ongoing neurodegeneration as it often precedes clinical worsening. Longitudinal neurodegenerative biomarkers in MS which predict clinical progression are required. Visual system biomarkers might serve as an attractive source for longitudinal neurodegenerative biomarkers as they have a direct link to a specific clinical outcome and are easy to access without causing any harm to the patients.

Visual impairment is one of the most prevalent symptoms of MS, has high impact on quality of life,[2] and is therapeutically approached[3]. Optical coherence tomography (OCT) can quantify integrity of the retinal nerve fiber layer (RNFL), the ganglion cell and inner plexiform layer (GCIPL), as well as the inner nuclear layer (INL) with high precision[4] and might also serve as a diagnostic tool in MS[5]. A reduction in RNFL and GCIPL has been observed in all subtypes of MS[6], is rather independent from inflammatory disease activity and seems to be accelerated in progressive MS.[7] Retinal layer atrophy has been associated with high and low contrast visual acuity, cortical atrophy[8] and cognitive impairment.[9] In progressive MS, reduced RNFL also seems to predict an increased risk of disability progression.[10] Thus, based on current knowledge, the visual system might be tightly associated with overall neurodegeneration in MS. While most of the studies analyzing the visual system included individuals with relapsing-remitting MS (RRMS), there are only few reported studies on PPMS, often with low participant numbers.[10–12] Moreover, most previous studies focused on specific outcomes such as single retinal layers and their correlations. To characterize and understand the dynamics of neurodegenerative processes and their impact on disability, multimodal longitudinal analysis of the visual system especially in progressive MS patients are urgently warranted.

Another biomarker that might represent neurodegeneration in MS is neurofilament light chain (NfL). NfL is one of the main components of the axonal cytoskeleton and axonal damage leads to a release into the cerebrospinal fluid and, to a lesser extent, into the serum where it can be measured with a single molecule array.[13] Many studies revealed that serum NfL (sNfL) levels are elevated in neurological diseases with neuroaxonal damage[14] and correlate with MRI activity and relapse rate in MS patients.[15] Although several studies show that sNfL levels are associated with indicators of disease worsening such as optic neuritis[16] and brain atrophy[17], it is still a matter of debate whether sNfL levels can predict long-term disability,[18] especially in progressive MS patients, where inflammatory activity is barely present.[19] It has been shown that the presence of both an elevated sNfL level and a reduced GCIPL volume presents a stronger risk factor for future disease activity than the presence of each marker individually[20] and that elevated sNfL levels are associated with higher retinal neuroaxonal loss in RRMS patients but not in progressive MS patients.[21] However, associations between visual outcomes and sNfL levels in progressive MS patients have not been explored, but are highly required to understand the MS disease specific mechanisms in the visual system.[22]

We hypothesize that visual systems biomarkers could serve as a prediction tool for clinical worsening in PPMS patients and are more precise than currently used predictive biomarkers as sNfL. In a large, longitudinal, observational cohort study on individuals with PPMS we here report for the first time on a multimodal analysis of advanced visual function outcomes, OCT, MRI, and sNFL levels in patients, together with a cross-sectional comparison with healthy controls.

MATERIALS AND METHODS

Participants

We included patients with PPMS from two observational cohorts between 2012 and 2018. Patients were either recruited at the multiple sclerosis outpatient clinic at the University Medical Centre Hamburg-Eppendorf (UKE), or at the NeuroCure Clinical Research Center, Charité – Universitätsmedizin Berlin, both Germany. Patients were eligible if they were diagnosed with PPMS according to the McDonald criteria 2010, had a maximum Expanded Disability Status Scale (EDSS) of 7.0 and were between 18 and 65 years old. Patients were excluded if they had major medical problems other than MS or a contraindication for MRI. Age-matched healthy controls were recruited at the UKE. All participants gave their written informed consent prior to any testing. The study was approved by the local ethics committee (Ethical Committee of the Board of Physicians Hamburg, PV4455, PV3961 and PV5557, Ethical Committee of the Charité, EA1/163/12).

Procedures

Patients in Hamburg were evaluated annually with the EDSS, the Timed 25 Foot Walk Test (T25WT), the Symbol Digit Modalities Test (SDMT) and the Nine Hole Peg Test (NHPT). Visual function was assessed on each eye separately using high-contrast visual acuity (HCVA) charts at 5 meters, and the complete contrast sensitivity function (CSF) measured by the quantitative CSF (qCSF) approach which is a computerized test using a Bayesian adaptive method to assess the full CSF.[23] Several features were calculated from the CSF, including the area under the log CSF (AULCSF), the CSF acuity (the point estimate at full contrast), and contrast sensitivities at individual spatial frequencies (1.5, 3, 6, 12 and 18 cycles per degree). Additionally, serum samples were collected at each visit. Healthy controls underwent a cross-sectional assessment including OCT, MRI and visual function without biosampling. Thus, an independent matched cohort of controls from the UKE biobank was used for comparison of

sNfL levels. Patients in Berlin were assessed on an annual basis for up to four years and only high contrast visual acuity (HCVA), OCT and EDSS were examined.

OCT protocol and processing

OCT scans were performed with the Spectralis SD-OCT (Heidelberg Engineering, Heidelberg, Germany, pupils not dilated, eye tracking). For measurement of the peripapillary retinal nerve fiber layer thickness (pRNFL) we used a ring scan around the optic nerve head (12°, 1536 A-scans, 16 ≤ ART ≤ 100) using the device-internal segmentation module 6.0.14.0. Ring scans in Hamburg before 2015 were performed with a slightly higher diameter (~3.5 vs. ~3.4mm) and excluded from the RNFL thickness analyses. A macular volume scan (25° × 30°, 61 B-scans, 768 A-scans per B-scan, 12 ≤ ART ≤ 15) quantified the retinal volume, ganglion cell and inner plexiform layer (GCIPL), and the inner nuclear layer (INL). Scans not meeting the OSCAR-IB consensus criteria[24] were excluded. The SAMIRIX pipeline[25] was used for intraretinal layer segmentation of the macula scans and volumes were extracted in a 3 mm diameter cylinder around the fovea. Layer segmentation was manually corrected by two experienced graders. Subclinical optic neuritis (sON) might be an important covariate and we defined an intraindividual RNFL thickness difference above 6µm as suggestive for sON.

MRI protocol and processing

The MRI protocol was performed for all subjects on the same scanner (Siemens Skyra 3T) and included a 3D T1-weighted magnetization-prepared rapid acquisition with gradient echo (TR = 1900 ms; TE = 2.46 ms; FA = 9°; voxel size = 0.9mm^3), a T2-weighted sequence (TR = 2800ms; TE = 18ms; FA = 160°; voxel size = 0.5 × 0.5 × 3 mm^3), a diffusion tensor imaging scan (single-shell, 20 directions with noncollinear diffusion gradients [b = 1,000 s/mm^2] and a non-diffusion-weighted b0 image (1.9 × 1.9 × 2.0 mm). Diffusion data were only available in 42 patients. We used the FreeSurfer software (surfer.nmr.mgh.harvard.edu) for calculating brain and grey matter volume adjusted for total intracranial volume. The TractSeg pipeline[26] was used for segmentation of four white matter bundles associated with the processing of

visual stimuli: Optic radiation (OR), parieto-occipital-pontine tract (POPT), superior longitudinal fascicle II (SLF_II) and thalamo-occipital tract (T_OCC). We extracted mean diffusivity (MD) values averaged over each tract as a proxy for structural integrity.

sNfL measurement

Blood samples were collected in standard serum tubes, aliquoted and stored at −80°C. All samples were shipped at –80°C to the University Hospital Basel, Switzerland. sNfL levels were determined using the single-molecule array (Simoa®; Quanterix, Lexington, MA, USA) assay.[27] We compared sNfL raw values in pg/ml from PPMS patients to healthy controls. sNfL Z Scores based on healthy controls were calculated as described previously.[27]

Statistical analysis

Descriptive statistics are presented as mean with standard deviation (SD), median with range or frequencies. Group differences and associations were evaluated with linear mixed effect (LME) models adjusted for repeated measurements and with random intercepts. All models were adjusted for age, sex, sON, and, when examining RNFL thickness, the OCT protocol. To describe the rate of abnormality, we computed percentile ranks based on the normative data from the control cohorts. To determine putative collapsing points of structural outcomes for visual function we used segmented regression adjusted for age, sex, and sON. Finally, we defined groups of patients with any and without any loss of visual function (AULCSF) during follow-up and we used ANOVAs to investigate a time x group interaction adjusted for age, sex, and sON for outcomes. P-values below 0.05 were considered statistically significant. All statistical analysis was performed with Statistics in R 4.2.1.

RESULTS

PPMS patients show retinal neuroaxonal loss, high sNfL serum levels and impaired visual functions despite a lack of clinical optic neuritis

81 patients with PPMS and two control cohorts (each n = 52) were enrolled in this study (T*able 1)*. Patients had a moderate disability level with a median EDSS of 3.5 (range 2.0 – 7.0). None of the participants reported a previous optic neuritis but 15 of 79 patients with values from both eyes (19%; 95%CI: 11 - 29%) and 5 of 44 controls (11%; 95%CI: 4 - 26%; p = 0.399) had a RNFL difference between eyes above 6µm which is suggestive of sON. The rate of sON in controls is compatible with the original cut-off definition based on the 95% CI of inter-eye differences from a previously published dataset including 31 healthy subjects.[5] Exploring density plots of eye differences for vision and OCT outcomes showed over all very similar distributions for patients and controls. Only retinal volume and RNFL showed a shift towards more asymmetry suggesting that a higher RNFL cut-off of 10 µm might be more suitable in PPMS (see supplementary **Figure SF1**). The mean follow-up time of patients was 2.7 years (SD: 1.7; up to 6 years). RNFL asymmetry increased during the follow-up in the entire cohort (+ 0.4 µm / year, p = 0.003) with a faster increase in those patients with an asymmetry at baseline (+ 1.0 µm / year, p = 0.005).

First, we compared differences of visual system biomarkers and sNfL between patients and controls (Table 2 and Figure 1). PPMS patients had an impaired visual function with reduced AULCSF and CSF acuity, while HCVA differences did not reach significance. We noticed a tendency of higher spatial frequencies to be statistically significantly impaired despite a probable floor effect at very high spatial frequencies (Figure 1 D and cycles per degree (CPD) results in Table 2). We observed lower thickness of pRNFL and GCIPL in the OCT of PPMS patients. Brain parenchymal fractions were not significantly reduced, while sNfL values were higher in PPMS patients than in controls. Eyes suggestive for sON showed worse visual functioning (AULCSF and CSF acuity) and had lower retinal layer volumes (Table 2). In PPMS,

sON was also associated with increased MD values in the thalamo-occipital tracts, indicating a loss of structural tract integrity (Table 2). However, sON was not related to sNfL values (Table 2). Aging was associated with a decrease in HCVA, total macula volume, GCIPL and INL thickness as well as in brain parenchymal fractions whereas NfL values increased with age (Table 2, Figure 1). Brain volume seemed to decrease faster in patients than in controls over the age range, what can be considered as a proxy of disease duration in our cohort, but the interaction group x age did not reach significance (p = 0.069).

Disease duration is not associated with visual function tests but with retinal neuronal layer loss

Next, we were interested how these parameters were related to disease duration (*Figure 2)*. We observed no significant association for the three visual function tests: HCVA (*p*=0.412), AULCSF (*p*=0.198) and CSF Acuity (*p*=0.531). Absolute sNfL levels were not correlated with disease duration (beta=-0.15, 95%CI: -0.42-0.11, *p*=0.291) but z-scores tended to decrease by 0.04/year (95%CI: 0-0.08, *p*=0.050).

The RNFL thickness decreased with disease duration by 0.55 µm/year (*95%CI: 0.13 - 0.96*; *p* = 0.010), the retinal volume by 0.006mm^3/y (95%CI: 0.002 - 0.010; *p* = 0.007) and the GCIPL volume by 0.004mm^3/y (*95%CI: 0.001 - 0.007, p* = 0.002). The change in INL volume did not reach significance (*p* = 0.700). MD increased in T_OCC by 0.06 x 10^{-3} mm^2/s for each year of disease duration (95%CI: 0 - 0.12, *p* = 0.037), whereas there was no association in the OR (p = 0.124), POPT (*p* = 0.369) and SLF_II (*p* = 0.484). Due to the co-linearity between age and disease duration, we recomputed all models without age as a covariate. However, this did not change the results relevantly.

We visualized the loss in average percentile rank in comparison to controls in *Figure 2M*. Only sNfL levels and INL volume were elevated at time of diagnosis while CSF acuity, RNFL thickness and GCIPL volume were already clearly reduced. GCIPL showed the most constant and clear decline. This indicates that a neuronal retinal layer loss precedes clinical visual functions by several years. Assuming a similar constant rate of GCIPL percentile rank loss

(0.9%/year) before diagnosis (mean percentile rank 32.8), we estimated the time when our cohort was at the 50 percentile on average, i.e. indistinguishable from controls. This silent onset of the disease was approximately 18 years before diagnosis (approximately 20 years based on RNFL thickness loss).

Loss of visual function presents at low retinal thickness values

Next, we investigated how neurodegeneration of the retina and tracts determines visual function. *Figure 3* shows that visual function tests are stable or decrease very little up to a certain point of structural integrity loss after which, there was a functional decrease associated with further neurodegeneration. Segmented regression determined these turning points of AULCSF stability at a RNFL thickness of 90.6µm (*Figure 3A*, *95%CI*: 84.9 - 96.3, $p < 0.001$), and a GCIPL volume of 0.43mm³ (*Figure 3B*, *95%CI*: 0.40 - 0.46, $p < 0.001$). AULCSF covering the whole spectrum of contrasts and spatial frequencies, seemed to decline faster (standardized *beta* = 0.89, $p = 0.010$) than high contrast outcomes (HCVA: standardized *beta* = 0.39, $p = 0.001$ and CSF Acuity: standardized *beta* = 0.79, $p < 0.001$). However, turning points for HCVA (RNFL: 92.1µm, GCIPL: 0.41mm^3) and CSF Acuity (RNFL: 91.7µm, GCIPL: 0.43mm^3) were similar as for AULCSF. Out of the tracts, SLF_II (*Figure 3C*) showed an accelerated functional loss above an MD threshold of 0.76 10^{-3} × mm^2/s (*95%CI*: 0.74 - 0.78, $p < 0.001$) for AULCSF. Only a very high borderline MD value indicated a functional loss in the T_OCC (*Figure 3D*, 1.25 10^3 × mm^2/s, *95%CI*: 0.74 - 0.78, $p < 0.001$), whereas OR and POPT showed no turning point. We found no cut-off value associated with sNfL z-scores. Associations between all outcomes are reported in detail in the supplemental material (*Figure SF2* and *Table ST1*).

AULCSF could serve as a prognostic tool for retinal thinning

As AULCSF seemed a more sensitive outcome to monitor visual function than HCVA and CSF Acuity, we analyzed whether other outcomes differed also between patients with a decline in AULCSF (individual beta coefficient AULCSF over time < 0, $n = 25$) or without ($n = 26$).

Patients with an AULCSF progression showed a decrease in HCVA (*beta* = -0.09 /y, *p* = 0.005) and CSF Acuity (*beta* = -0.03 /y, *p* = 0.007). The change in sNfL was similar in both groups (*p* = 0.378). EDSS increased faster in patients with AULCSF progression (*beta* = 0.17 /y, *p* = 0.043), while NHPT (*p* = 0.939), T25FW (*p* = 0.172) and SDMT (*p* = 0.790) dynamics did not differ between groups. The loss in RNFL (p = 0.666) and retinal volume (*p* = 0.523) did not differ between the groups. GCIPL decreased less in progressors than in stable patients (*beta*=0.004 mm^3/year, p = 0.028) while INL volume remained stable in both groups (*p* = 0.611). Changes in MD values from tracts did not differ between groups.

Discussion

Our study revealed the predictive potential of visual system biomarkers for clinical worsening in PPMS. We detected a temporarily preserved visual function despite an early and ongoing reduction of visual structural integrity in PPMS. Importantly, retinal neurodegeneration and active neuronal loss as indicated by high sNfL levels at the diagnosis of the disease support a pre-clinical neurodegeneration over several years.

Our large, multidimensional and longitudinal data set confirmed cross-sectional observations that PPMS patients have a significantly lower RNFL thickness, GCIPL volume and a trend towards a lower retinal volume when compared with healthy controls.[7] Compared to a younger cohort of 333 RRMS with a comparable disease duration below 10 years, RNFL thickness in our PPMS cohort of ~91 µm was more similar to patients without a history of ON (~92 µm) than to patients with a history of ON (~83µm).[28] Here, every year of disease duration was associated with a RNFL thickness loss of approximately 0.55 µm/year which is rather similar to an ON independent rate of RNFL loss in the same RRMS cohort of 1.76 µm over 36 months or in other cohorts of 1.1 µm over 2 years.[28,29] Thus, continuous RNFL thickness loss in RRMS and PPMS seems very similar if independent from inflammatory ON activity, i.e., it seems to represent rather ongoing neurodegeneration than acute inflammation. This conclusion might also explain why we did not observe an INL increase, which has previously been reported as a surrogate of inflammation in MS.[30] Moreover, our results underline that the association between retinal damage and visual function is not linear. We were able to determine turning points, for example once pRNFL thickness falls below 92.1µm, retinal neurodegeneration begins to translate into faster, progressive visual function impairment as defined by the AULCSF. This is much higher than previously reported turning points of 60 µm for MS and other neuroinflammatory diseases using standard visual acuity charts.[31] Persisting high contrast visual impairment after ON was previously only observed below a threshold of 75µm RNFL thickness[32]. Interestingly, subclinical ON (sON) - as defined by the recently promoted 6 µm inter-eye difference cut-off - was present in one out of five patients in our cohort and one

out of 10 healthy controls. Given the expected rate of zero optic neuritis in both groups, the current definition seems not sufficiently sensitive and specific in our cohort. Our analysis revealed that a higher cut-off of around 10 µm might be more suitable, but this needs further investigations. In addition, it might be interesting to also study the longitudinal dynamic of inter-eye asymmetry, for RNFL but also for other outcomes. However, the 6µm sON definition showed a moderate association with CSF outcomes but had no relevant association with other outcomes in our cohort. This observation might underline the hypothesis that PPMS has a rather diffuse, sometimes asymmetric, neurodegenerative pathophysiology with a less focal lesioning aspect than relapsing-remitting MS. Moreover, asymmetry in PPMS might be less driven by silent optic neuritis but through imbalanced brain atrophy that translates via retrograde transsynaptic degeneration from nonprimary visual areas into the retina.[33] Our findings support the robustness of the visual system against neuronal damage in PPMS, which might be partially explained by functional reorganization of information processing beyond primary visual areas and consecutive structural reorganization.[34] The long preclinical phase despite proven substantial retinal damage in PPMS might thus hint towards a more resilient brain network architecture or physiology in comparison to other disease courses.

We found a distinct association between atrophy of the pRNFL, GCIPL and retinal volume and a worsening of the vision parameters but no association between INL and clinical outcomes. Assessments using the complete contrast sensitivity function detected mild visual impairment earlier in the disease course than standard HCVA. The higher sensitivity of low contrast visual acuity has been reported before, could be confirmed here by analyzing different features derived from the CSF estimate, and its relevance is underlined by better correlation with important health dimensions like participation or activities of daily living.[35] Despite the similarity of a pronounced impairment of low contrast vision in RRMS and PPMS, reference data comparing contrast sensitivity and retinal integrity is lacking. Moreover, our analyses provide further evidence for trans-synaptic and downstream degeneration and its link to higher order functions.[36,37] Here, advanced anterior visual system impairment correlated with increased

diffusivity, a sensitive marker of neuronal tract integrity, that links vision to other functional systems, namely a cognitive task measuring information processing.[38]

When investigating progression and outcome dynamics, we observed a more complex picture. In patients with a stable AULCSF over the disease course, the reduction of GCIPL volume was higher than in patients with AULCSF progression. This might be explained by the robustness of visual functioning against structural damage, already mentioned and discussed above. However, AULCSF progressors also had a faster increase in EDSS. Overall, our findings underline the heterogeneity of multiple sclerosis disability patterns in PPMS, the need for a precise disability assessment on an individual level and the advantage of multimodal studies.

In comparison to most other studies, we were able to evaluate the association of these changes with disability outcomes, MRI parameters and the levels of sNfL in a longitudinal setting. Over up to five years, we observed a homogeneous and constant thinning of retinal nerve layers and elevation of sNfL levels, indicating a rather constant rate of neurodegeneration in our cohort. Here, we did not observe a strong association between retinal atrophy and sNfL. Larger longitudinal data sets in PPMS might allow advanced modelling of associations including other disease characteristics and cofounders of NfL levels like overall disability, lesions, spinal cord atrophy or body mass index. The highest sNfL values were detected at the beginning of the disease, followed by high and stable sNfL levels during follow-up. As sNfL concentrations increase with age,[39] we used z-scores which reflect the deviation to a control cohort.[40] Current studies in multiple sclerosis show a strong association of sNfL with inflammatory activity in multiple sclerosis, while the increase specific to disease progression appears more subtle.[18,41–44] Many studies have shown associations between sNfL levels and clinical outcomes,[41,43,45] and it was also shown that NfL levels in the CSF at the onset of optic neuritis predict low contrast visual acuity, RNFL and GCIPL at follow-up.[16] Here, we could not detect any association between visual outcomes and sNfL levels, which might be explained by the presence of sNfL derived from neuronal damage outside of the visual

system introducing variability. Moreover, sNfL levels did not differ between patients with stable or unstable AULCSF during the disease. However, follow-up studies including more patients with a longer disease duration are needed.

Our study has several limitations. Despite our cohort being rather large, understanding disease mechanisms in a pathology that acts over decades remains restricted. We also aimed to correlate the interaction between structure and function, but informative outcomes such as visual evoked potentials and functional MRI were not included in the design of the study. These would have allowed the determination of functional integrity and functional compensation, putative important mediators between structural damage and real-life performance. The lack of diffusion imaging in controls made a comparison of downstream structural connectivity of important brain tracts impossible. Also, the lack of longitudinal data for controls restricts the interpretability of longitudinal data in PPMS as normal aging effects are not robustly captured in the cross-sectional comparison. Finally, our analyses are possibly limited by a variability and potential bias introduced by combining different datasets from two centers with two different control cohorts for sNfL and visual system.

In summary, we identified that visual function in people with PPMS is rather robust against neurodegeneration of retinal layers which is already present at the beginning of the disease. Interestingly, sNfL levels were not associated with visual function or thinning of retinal layers, while OCT and AULCSF could prove their usefulness in detecting neurodegeneration. The easy and highly precise multimodal assessment of its integrity might allow a personalized disease surveillance, prognosis and monitoring of putative neuroregenerative treatments in the future.

Acknowledgements

We thank all colleagues of the INIMS biobank.

Funding

Initial setup by unrestricted grants from Novartis and MerckSerono. SCR is supported by a Clinician-Scientist Fellowship from the Hertie Network of Excellence in Clinical Neuroscience of the Gemeinnützige Hertie-Stiftung.

Diversity statement

Recent work in several fields of science has identified a bias in citation practices such that papers from women and other minority scholars are under-cited relative to the number of such papers in the field. Here we sought to proactively consider choosing references that reflect the diversity of the field in thought, form of contribution, gender, race, ethnicity, and other factors. Using the CleanBib approach (https://github.com/dalejn/cleanBib), we obtained first the predicted gender of the first and last author of each reference by using databases that store the probability of a first name being carried by a woman. By this measure and excluding self-citations to the first and last authors of our current paper), our references contain 12.82% woman(first)/woman(last), 15.38% man/woman, 12.2% woman/man, and 59.6% man/man. This method is limited in that a) names, pronouns, and social media profiles used to construct the databases may not, in every case, be indicative of gender identity and b) it cannot account for intersex, non-binary, or transgender people. Second, we obtained predicted racial/ethnic category of the first and last author of each reference by databases that store the probability of a first and last name being carried by an author of color. By this measure (and excluding self-citations), our references contain 11.34% author of color (first)/author of color(last), 14.92% white author/author of color, 23.26% author of color/white author, and 50.48% white author/white author. This method is limited in that a) names and Florida Voter Data to make the predictions may not be indicative of racial/ethnic identity, and b) it cannot account for Indigenous and mixed-race authors, or those who may face differential biases due to the ambiguous racialization or ethnicization of their names. See also supplemental material for

more extensive information about our citations. We look forward to future work that could help us to better understand how to support equitable practices in science.

Competing interests

SCR - nothing to declare

LG – nothing to declare.

ACH – nothing to declare.

MD – has financial and intellectual property interests in and holds employment by Adaptive Sensory Technology.

VH – nothing to declare.

ML – nothing to declare.

SR – nothing to declare.

JK – nothing to declare.

CH – nothing to declare

MAF – has received honoraria as speaker and for consultation from Biogen, Lundbeck, Merck KGaA, Novartis and Roche. His research is funded by the Bundesministerium für Bildung und Forschung (BMBF), Deutsche Forschungsgemeinschaft (DFG), Landesforschungsförderung Hamburg, Gemeinnützige Hertie-Stiftung, Else Kröner-Fresenius-Stiftung, Fritz Thyssen-Stiftung, Werner Otto-Stiftung and Deutsche Multiple Sklerose-Gesellschaft.

AB – nothing to declare

FP - nothing to declare

HGZ – received speaking honoraria from Bayer Healthcare and Novartis and research grants from Novartis.

JPS – nothing to declare.

References

1. Faissner S, Plemel JR, Gold R, Yong VW. Progressive multiple sclerosis: from pathophysiology to therapeutic strategies. *Nat Rev Drug Discov*. 2019;18(12):905-922. doi:10.1038/s41573-019-0035-2

2. Balcer LJ, Miller DH, Reingold SC, Cohen J a. Vision and vision-related outcome measures in multiple sclerosis. *Brain*. 2015;138(Pt 1)(Jan):11-27. doi:10.1093/brain/awu335

3. Lagrèze WA, Küchlin S, Ihorst G, et al. Safety and efficacy of erythropoietin for the treatment of patients with optic neuritis (TONE): a randomised, double-blind, multicentre, placebo-controlled study. *Lancet Neurol*. 2021;20(12):991-1000. doi:10.1016/s1474-4422(21)00322-7

4. Petzold A, Balcer L, Calabresi PA, et al. Retinal layer segmentation in multiple sclerosis: a systematic review and meta-analysis. *Lancet Neurol*. 2017;16(10):797-812. doi:10.1016/S1474-4422(17)30278-8

5. Petzold A, Chua SYL, Khawaja AP, et al. Retinal asymmetry in multiple sclerosis. *Brain*. 2021;144(1):224-235. doi:10.1093/brain/awaa361

6. Martinez-lapiscina EH, Arnow S, Wilson JA, et al. Retinal thickness measured with optical coherence tomography and risk of disability worsening in multiple sclerosis : a cohort study. *Lancet Neurol*. 2016;4422(16):1-11. doi:10.1016/S1474-4422(16)00068-5

7. Sotirchos ES, Gonzalez Caldito N, Filippatou A, et al. Progressive Multiple Sclerosis Is Associated with Faster and Specific Retinal Layer Atrophy. *Ann Neurol*. 2020;87(6):885-896. doi:10.1002/ana.25738

8. Saidha S, Sotirchos ES, Oh J, et al. Relationships between retinal axonal and neuronal measures and global central nervous system pathology in multiple sclerosis. *JAMA Neurol*. 2013;70(1):34-43. doi:10.1001/jamaneurol.2013.573

9. Ko F, Muthy ZA, Gallacher J, et al. Association of Retinal Nerve Fiber Layer Thinning with Current and Future Cognitive Decline: A Study Using Optical Coherence Tomography. *JAMA Neurol*. 2018;75(10):1198-1205. doi:10.1001/jamaneurol.2018.1578

10. Martinez-Lapiscina EH, Arnow S, Wilson JA, et al. Retinal thickness measured with optical coherence tomography and risk of disability worsening in multiple sclerosis: A cohort study. *Lancet Neurol*. 2016;15(6):574-584. doi:10.1016/S1474-4422(16)00068-5

11. Pisa M, Ratti F, Vabanesi M, et al. Subclinical neurodegeneration in multiple sclerosis and neuromyelitis optica spectrum disorder revealed by optical coherence tomography. *Mult Scler J*. 2020;26(10):1197-1206. doi:10.1177/1352458519861603

12. Klumbies K, Rust R, Dörr J, et al. Retinal Thickness Analysis in Progressive Multiple Sclerosis Patients Treated With Epigallocatechin Gallate: Optical Coherence Tomography Results From the SUPREMES Study. *Front Neurol*. 2021;12(April):1-9. doi:10.3389/fneur.2021.615790

13. Kuhle J, Barro C, Andreasson U, et al. Comparison of three analytical platforms for quantification of the neurofilament light chain in blood samples: ELISA, electrochemiluminescence immunoassay and Simoa. *Clin Chem Lab Med*. 2016;54(10):1655-1661. doi:10.1515/cclm-2015-1195

14. Khalil M, Teunissen CE, Otto M, et al. Neurofilaments as biomarkers in neurological disorders. *Nat Rev Neurol*. 2018;14(10):577-589. doi:10.1038/s41582-018-0058-z

15. Kuhle J, Barro C, Disanto G, et al. Serum neurofilament light chain in early relapsing

remitting MS is increased and correlates with CSF levels and with MRI measures of disease severity. *Mult Scler*. 2016;22(12):1550-1559. doi:10.1177/1352458515623365

16. Modvig S, Degn M, Sander B, et al. Cerebrospinal fluid neurofilament light chain levels predict visual outcome after optic neuritis. *Mult Scler*. 2016;22(5):590-598. doi:10.1177/1352458515599074

17. Barro C, Benkert P, Disanto G, et al. Serum neurofilament as a predictor of disease worsening and brain and spinal cord atrophy in multiple sclerosis. *Brain*. 2018;141(8):2382-2391. doi:10.1093/brain/awy154

18. Bittner S, Oh J, Havrdová EK, Tintoré M, Zipp F. The potential of serum neurofilament as biomarker for multiple sclerosis. *Brain*. June 2021. doi:10.1093/brain/awab241

19. Kuhle J, Plavina T, Barro C, et al. Neurofilament light levels are associated with long-term outcomes in multiple sclerosis. *Mult Scler*. 2020;26(13):1691-1699. doi:10.1177/https

20. Lin TY, Vitkova V, Asseyer S, et al. Increased Serum Neurofilament Light and Thin Ganglion Cell-Inner Plexiform Layer Are Additive Risk Factors for Disease Activity in Early Multiple Sclerosis. Neurol Neuroimmunol neuroinflammation. 2021;8(5). doi:10.1212/NXI.0000000000001051

21. Sotirchos ES, Vasileiou ES, Filippatou AG, et al. Association of Serum Neurofilament Light Chain with Inner Retinal Layer Thinning in Multiple Sclerosis. *Neurology*. 2022;99(7):E688-E697. doi:10.1212/WNL.0000000000200778

22. Costello F. Erythropoietin and optic neuritis in the TONE study. Lancet Neurol. 2021;20(12):970-971. doi:10.1016/s1474-4422(21)00378-1

23. Rosenkranz SC, Kaulen B, Zimmermann HG, Bittner AK, Dorr M, Stellmann JP. Validation of Computer-Adaptive Contrast Sensitivity as a Tool to Assess Visual Impairment in Multiple Sclerosis Patients. *Front Neurosci*. 2021;15(February):1-8.

doi:10.3389/fnins.2021.591302

24. Tewarie P, Balk L, Costello F, et al. The OSCAR-IB Consensus Criteria for Retinal OCT Quality Assessment. *PLoS One*. 2012;7(4):e34823. doi:10.1371/journal.pone.0034823

25. Motamedi S, Gawlik K, Ayadi N, et al. Normative Data and Minimally Detectable Change for Inner Retinal Layer Thicknesses Using a Semi-automated OCT Image Segmentation Pipeline. Front Neurol. 2019;10(November):1-10. doi:10.3389/fneur.2019.01117

26. Wasserthal J, Neher P, Maier-Hein KH. TractSeg - Fast and accurate white matter tract segmentation. *Neuroimage*. 2018;183(August):239-253. doi:10.1016/j.neuroimage.2018.07.070

27. Sutter R, Hert L, De Marchis GM, et al. Serum Neurofilament Light Chain Levels in the Intensive Care Unit: Comparison between Severely Ill Patients with and without Coronavirus Disease 2019. *Ann Neurol*. 2021;89(3):610-616. doi:10.1002/ana.26004

28. Paul F, Calabresi PA, Barkhof F, et al. Optical coherence tomography in multiple sclerosis: A 3-year prospective multicenter study. *Ann Clin Transl Neurol*. 2021;(May):1-17. doi:10.1002/acn3.51473

29. Balk LJ, Cruz-Herranz A, Albrecht P, et al. Timing of retinal neuronal and axonal loss in MS: a longitudinal OCT study. *J Neurol*. 2016;263(7):1323-1331. doi:10.1007/s00415-016-8127-y

30. Balk LJ, Coric D, Knier B, et al. Retinal inner nuclear layer volume reflects inflammatory disease activity in multiple sclerosis; a longitudinal OCT study. *Mult Scler J - Exp Transl Clin*. 2019;5(3). doi:10.1177/2055217319871582

31. Gigengack NK, Oertel FC, Motamedi S, et al. Structure–function correlates of vision loss in neuromyelitis optica spectrum disorders. *Sci Rep*. 2022;12(1):1-11. doi:10.1038/s41598-022-19848-4

32. Costello F, Coupland S, Hodge W, et al. Quantifying axonal loss after optic neuritis with optical coherence tomography. *Ann Neurol*. 2006;59(6):963-969. doi:10.1002/ana.20851

33. Stellmann J-P, Cetin H, Young KL, et al. Pattern of gray matter volumes related to retinal thickness and its association with cognitive function in relapsing-remitting MS. *Brain Behav*. 2017;7(2):e00614. doi:10.1002/brb3.614

34. Backner Y, Kuchling J, Massarwa S, et al. Anatomical Wiring and Functional Networking Changes in the Visual System Following Optic Neuritis. *JAMA Neurol*. 2018;75(3):287-295. doi:10.1001/jamaneurol.2017.3880

35. Balcer LJ, Raynowska J, Nolan R, et al. Validity of low-contrast letter acuity as a visual performance outcome measure for multiple sclerosis. *Mult Scler J*. 2017;23(5):734-747. doi:10.1177/1352458517690822

36. Berman S, Backner Y, Krupnik R, et al. Conduction delays in the visual pathways of progressive multiple sclerosis patients covary with brain structure. *Neuroimage*. 2020;221(July):117204. doi:10.1016/j.neuroimage.2020.117204

37. Gabilondo I, Martínez-Lapiscina E, Martínez-Heras E, et al. Trans-synaptic axonal degeneration in the visual pathway in Multiple Sclerosis. *Ann Neurol*. 2014;75(1):98-107. doi:10.1002/ana.24030

38. Menegaux A, Bäuerlein FJB, Vania A, et al. Linking the impact of aging on visual short-term memory capacity with changes in the structural connectivity of posterior thalamus to occipital cortices. Neuroimage. 2020;208(October 2019). doi:10.1016/j.neuroimage.2019.116440

39. Khalil M, Pirpamer L, Hofer E, et al. Serum neurofilament light levels in normal aging and their association with morphologic brain changes. *Nat Commun*. 2020;11(1):1-9. doi:10.1038/s41467-020-14612-6

40. Benkert P, Meier S, Schaedelin S, et al. Serum neurofilament light chain for individual prognostication of disease activity in people with multiple sclerosis: a retrospective modelling and validation study. *Lancet Neurol*. 2022;21(3):246-257. doi:10.1016/S1474-4422(22)00009-6

41. Williams T, Zetterberg H, Chataway J. Neurofilaments in progressive multiple sclerosis: a systematic review. J Neurol. 2021;268(9):3212-3222. doi:10.1007/s00415-020-09917-x

42. Leppert D, Kropshofer H, Häring DAA, et al. Blood Neurofilament Light in Progressive Multiple Sclerosis: Post Hoc Analysis of 2 Randomized Controlled Trials. *Neurology*. April 2022:10.1212/WNL.0000000000200258. doi:10.1212/WNL.0000000000200258

43. Kapoor R, Smith KE, Allegretta M, et al. Serum neurofilament light as a biomarker in progressive multiple sclerosis. *Neurology*. 2020;95(10):436-444. doi:10.1212/WNL.0000000000010346

44. Barro C, Healy BC, Liu Y, et al. Serum GFAP and NfL Levels Differentiate Subsequent Progression and Disease Activity in Patients With Progressive Multiple Sclerosis. *Neurol - Neuroimmunol Neuroinflammation*. 2023;10(1):e200052. doi:10.1212/nxi.0000000000200052

45. Abdelhak A, Cordano C, Boscardin WJ, et al. Plasma neurofilament light chain levels suggest neuroaxonal stability following therapeutic remyelination in people with multiple sclerosis. *J Neurol Neurosurg Psychiatry*. June 2022. doi:10.1136/jnnp-2022-329221

Table 1: Descriptive statistics.

	PPMS patients (n = 81)	Healthy controls vision (n = 52)	Healthy controls sNfL (n = 52)
Sex (female/male) n (%)	24/57 (29.7/70.3%)	36/16 (69.2/30.8) p<0.001	25/27 (48.1/51.9) p=0.338
Age y	51.8 (36.0-69.0; SD: 7.7)	50.2 (37.0–63.0; SD: 7.6) p=0.244	50.2 (31.0-63.0; SD: 7.2) p=0.025
Disease duration since diagnosis y	5.9 (0-20.2; SD: 5.8)		
Center (Hamburg /Berlin) n	64/17		
Follow up y	2.7 (0-6.2; SD: 1.7)		
Number of visits per patient Hamburg median [range] Berlin median [range]	 4 [2 – 6] 3 [1 - 7]		
EDSS median [range]	3.5 [2.0-7.0]		
T25FW sec	5.9 (3.2-14.3; SD: 2.2)		
NHPT sec	25.9 (17.1-55.8; SD: 7.7)		
SDMT correct answers	47.7 (17-80; SD:12.2)		
SDMT SD	-0.57 (-3.0-2.5; SD: 1.24)		
Immunotherapies at baseline	Ocrelizumab: n = 1 Mitoxantrone n = 1 β-interferons n =2		
New Immunotherapies during follow up	Rituximab / Ocrelizumab: n = 1 after 1y and n = 3 after 4 years Cladribine: n = 1 after 2 years		

PPMS = primary progressive MS; y = years; EDSS = expanded disability status scale; T25FW = timed 25-foot walk; sec = seconds; NHPT = nine-hole peg test, SDMT = symbol digit modalities test. SD = standard deviation in comparison to a normative cohort of healthy individuals. Data are presented as means (range; standard deviation) unless otherwise indicated.

Table 2: Comparison of vision, retinal layers and MRI parameters in PPMS patients and healthy controls.

	PPMS patients (n = 81) 153 eyes	Healthy controls (n = 52) 91 eyes				
	Cohort effect: Estimate (95%CI)	Cohort effect: Estimate (95%CI)	Effects	Estimate	95%CI	p
VISION						
HCVA N = 123 Observations = 531	0.80 (0.75-0.85)	0.89 (0.80-0.98)	PPMS	-0.092	-0.197 – 0.012	0.084
			Age	-0.078	-0.134 – -0.022	0.006*
			Male	0.034	-0.061 – 0.130	0.479
			sON	-0.026	-0.105 – 0.053	0.523
AULCSF N = 104 Observations = 430	1.17 (1.11-1.22)	1.26 (1.19-1.33)	PPMS	-0.096	-0.190 – -0.001	0.047*
			Age	-0.002	-0.053 – 0.049	0.939
			Male	0.031	-0.059 – 0.121	0.502
			sON	-0.062	-0.117 – -0.007	0.027*
CSF Acuity N = 104 Observations = 430	1.29 (1.26-1.32)	1.37 (1.32-1.41)	PPMS	-0.075	-0.131 – -0.020	0.007*
			Age	0.005	-0.025 – 0.035	0.754
			Male	0.007	-0.046 – 0.059	0.799
			sON	-0.045	-0.080 – -0.010	0.012*
Contrast sensitivity at 1.5 CPD N = 104 Observations = 430	1.33 (1.29-1.31)	1.36 (1.31-1.41)	PPMS	-0.029	-0.099 – 0.042	0.428
			Age	-0.014	-0.053 – 0.024	0.469
			Male	0.028	-0.039 – 0.095	0.405
			sON	-0.038	-0.083 – 0.007	0.100
Contrast sensitivity at 3 CPD N = 104 Observations = 430	1.38 (1.33-1.43)	1.42 (1.37-1.49)	PPMS	-0.047	-0.128 – 0.033	0.249
			Age	-0.004	-0.048 – 0.039	0.844
			Male	0.022	-0.055 – 0.099	0.569
			sON	-0.042	-0.090 – 0.005	0.079
Contrast sensitivity at 6 CPD N = 104 Observations = 430	1.18 (1.23-1.24)	1.29 (1.21-1.37)	PPMS	-0.105	-0.209 – -0.000	0.049*
			Age	0.011	-0.045 – 0.067	0.700
			Male	0.028	-0.072 – 0.127	0.581
			sON	-0.080	-0.140 – -0.020	0.010*
Contrast sensitivity at 12 CPD N = 104 Observations = 430	0.64 (0.58-0.71)	0.78 (0.70-0.87)	PPMS	-0.143	-0.256 – -0.030	0.014*
			Age	-0.006	-0.068 – 0.055	0.838
			Male	0.032	-0.075 – 0.139	0.562
			sON	-0.075	-0.152 – 0.003	0.058
Contrast sensitivity at 18 CPD N = 104 Observations = 430	0.24 (0.19-0.29)	0.36 (0.29-0.42)	PPMS	-0.114	-0.203 – -0.024	0.013*
			Age	-0.020	-0.070 – 0.029	0.417
			Male	0.042	-0.043 – 0.126	0.332
			sON	-0.039	-0.104 – 0.025	0.232
OCT						
Peripapillary RNFL thickness *µm* N = 110	90.6 (87.9-93.3)	97.3 (93.7-100.8)	PPMS	-6.647	-11.249 – -2.045	**0.005**
			Age	-2.183	-4.294 – -0.072	**0.043**
			Male	-2.015	-6.491 – 2.462	0.377
			sON	-8.590	-9.697 – -7.483	**<0.001**

Observations = 402						
Retinal volume (3mm circle macula) *mm³* N = 98 Observations = 436	2.35 (2.32-2.37)	2.38 (2.35-2.42)	PPMS	-0.039	-0.088 – 0.010	0.116
			Age	-0.040	-0.059 – -0.022	<0.001*
			Male	0.036	-0.012 – 0.083	0.137
			sON	-0.028	-0.039 – -0.017	<0.001*
GCIPL volume (3mm circle macula) *mm³* N = 115 Observations = 539	0.56 (0.54-0.57)	0.61 (0.59-0.64)	PPMS	-0.057	-0.086 – -0.027	<0.001*
			Age	-0.012	-0.023 – -0.000	0.041*
			Male	0.002	-0.026 – 0.030	0.902
			sON	-0.029	-0.036 – -0.022	<0.001*
INL volume (3mm circle macula) *mm³* N = 114 Observations = 533	0.298 (0.293-0.303)	0.290 (0.282-0.297)	PPMS	0.008	-0.001 – 0.017	0.078
			Age	-0.007	-0.011 – -0.003	0.001*
			Male	0.005	-0.004 – 0.013	0.273
			sON	0.005	0.002 – 0.008	0.002*
Subclinical optic neuritis: yes/no n (%)	15/64 (19.0/71.0%)	5/39 (11.4/88.6%)				
MRI						
Brain parenchymal fraction N = 77 Observations = 211	0.755 (0.746-0.763)	0.762 (0.746-0.777)	PPMS	-0.007	-0.025 – 0.012	0.468
			Age	-0.015	-0.022 – -0.008	<0.001*
			Male	-0.001	-0.017 – 0.015	0.924
			sON	-0.001	-0.007 – 0.005	0.759
Grey Matter fraction N = 77 Observations = 211	0.419 (0.413-0.425)	0.409 (0.397-0.420)	PPMS	0.010	-0.003 – 0.023	0.119
			Age	-0.012	-0.017 – -0.007	<0.001*
			Male	-0.008	-0.019 – 0.004	0.198
			sON	0.000	-0.004 – 0.004	0.865
Optic radiation (OR) *MD* N = 44 Observations = 87	0.791 (0.568-1.014)		Age	0.023	-0.016 – 0.061	0.245
			Male	-0.000	-0.074 – 0.074	0.996
			sON	0.028	-0.007 – 0.063	0.111
Parieto-occipital pontine (POPT) *MD* N = 39 Observations = 73	0.735 (0.615-0.855)		Age	0.015	-0.006 – 0.036	0.155
			Male	0.008	-0.026 – 0.042	0.628
			sON	0.010	-0.019 – 0.039	0.507
Superior longitudinal fascicle II (SLF_II) *MD* N = 46 Observations = 98	0.700 (0.630-0.771)		Age	0.010	-0.002 – 0.022	0.112
			Male	-0.014	-0.036 – 0.009	0.234
			sON	0.007	-0.007 – 0.020	0.342
Thalamo-occipital (T_OCC) *MD* N = 45 Observations = 91	0.753 (0.524-0.981)		Age	0.031	-0.009 – 0.070	0.127
			Male	0.019	-0.054 – 0.092	0.603
			sON	0.050	0.010 – 0.091	0.015*
sNfL						
sNfL pg/ml N = 116	12.0 (11.0-13.0)	8.4 (6.9-9.9)§	PPMS	3.572	1.749 – 5.396	<0.001*
			Age	1.942	0.785 – 3.099	0.001*
			sON	1.041	-1.190 – 3.272	0.359

Observations = 296						
sNfL z-scores N = 116 Observations = 296	0.99 (0.75-1.24)	0.07 (-0.23-0.37)§	PPMS	0.923	0.535 – 1.312	<0.001*
			sON	0.291	-0.039 – 0.621	0.083
sNfL percentiles N = 116 Observations = 296	74.3 (68.0-80.6)	53.2 (45.6-60.8)	PPMS	21.111	11.219 – 31.004	<0.001*
			sON	5.833	-2.192 – 13.858	0.154

Overview of altered visual system outcomes in PPMS compared to healthy controls. Effects and their 95%CI are from linear mixed effects models with cohort, age, sex and subclinical optic neuritis (sON) as explanatory variables. For major brain tracts, data from controls was not available. Number of eyes = number of available RNFL values at baseline. PPMS = primary progressive MS; HCVA = high contrast visual acuity; AULCSF = area under the log contrast sensitivity function; CSF Acuity = contrast sensitivity function acuity; CPD = cycles per degree; OCT = optical coherence tomography; RNFL = retinal nerve fibre layer; GCIPL = combined ganglion cell and inner plexiform layer; INL = inner nuclear layer; MD = mean diffusivity in $10^3 \times mm^2/s$; sNfL = serum neurofilament light chain. Brain and Gray matter volumes are divided by the intracranial volume providing parenchymal fractions. § = Independent healthy control cohort for sNfL comparison. Estimate of age effects reported as changes per decade.

Figures

Figure 1: Vision, retinal layers, brain volumes and tracts in PPMS and healthy controls

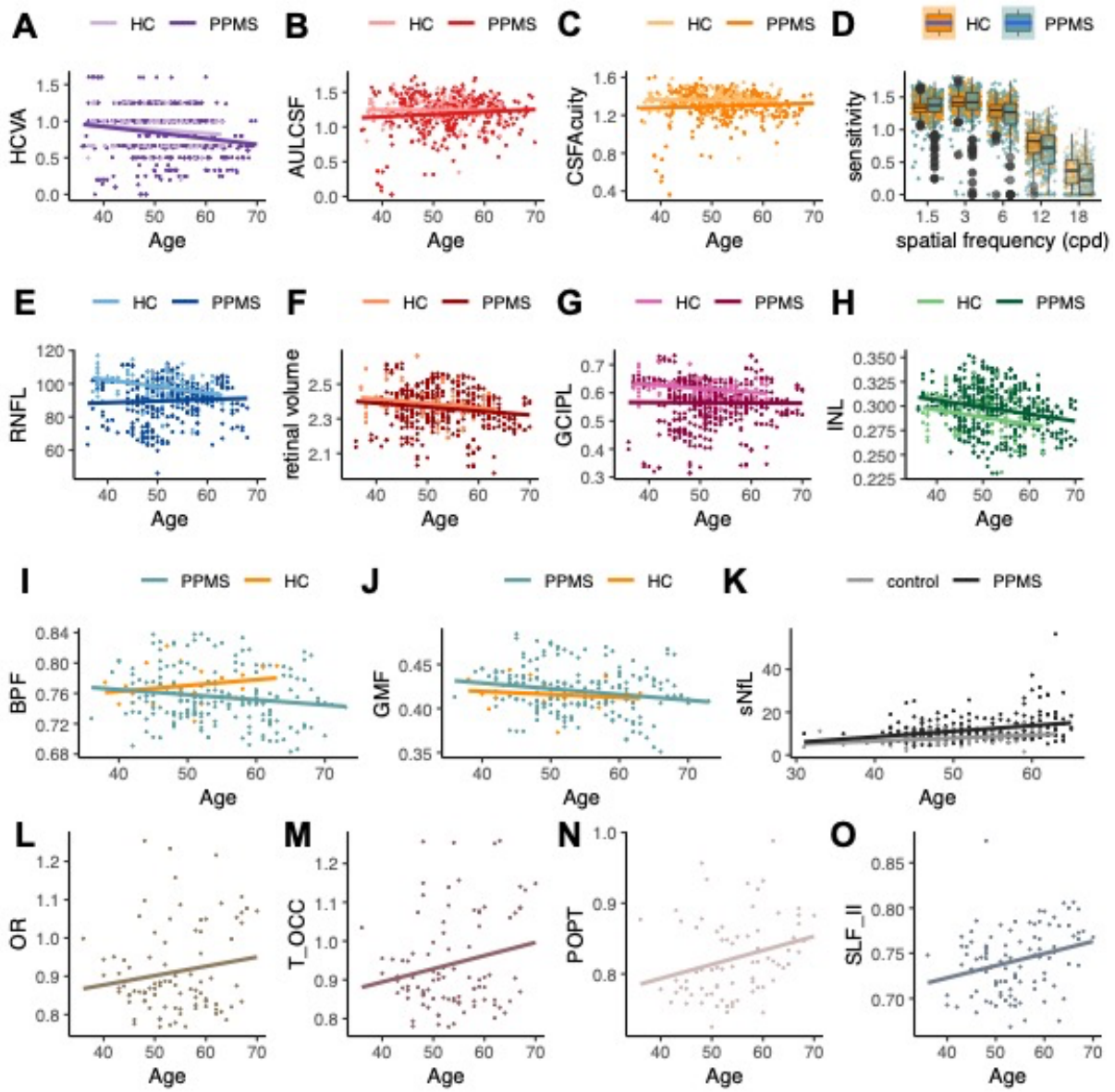

Dotplots with linear regression estimates (HC = healthy controls) illustrate age corrected differences between the groups and a putative different dynamic between the group – as for example for brain parenchymal fraction (BPF), which remains rather stable in controls between 40 and 60 years of age while there is a decrease in PPMS widening the gap between patient and controls at higher age. Figures are for illustrative purposes only and include all available data, i.e., recurrent assessments for patients. For estimates and statistics please refer to Table 2 with linear mixed effects models results adjusting for age, sex and intraindividual correlations. Visual function tests (**A-C**), Boxplots illustrating differences

in contrast sensitivity at different contrast levels between patients controls **(D)**, retinal layers (**D-G**), BPF (**H**), GMF = grey matter fraction (**I**), absolute serum neurofilament light levels (sNfL) in pg/ml (**J**) and tracts in the visual system (**K-N**). Mean diffusivity values for tracts (**K-N**) were only available from a subset (n = 42) of patients. HC = healthy controls; PPMS = primary progressive MS; HCVA = high contrast visual acuity; AULCSF = area under the log contrast sensitivity function; CSF Acuity = contrast sensitivity function acuity; CPD = cycles per degree; RNFL = retinal nerve fibre layer; GCIPL = combined ganglion cell and inner plexiform layer; INL = inner nuclear layer; sNfL = serum neurofilament light chain; OR = optic radiation; T_OCC: thalamo-occipital tract; POPT: parieto-occipital-pontine tract; SLF_II: superior longitudinal fascicle II.

Figure 2: Changes in vision, sNfL levels, retinal layers, and tracts over the disease course

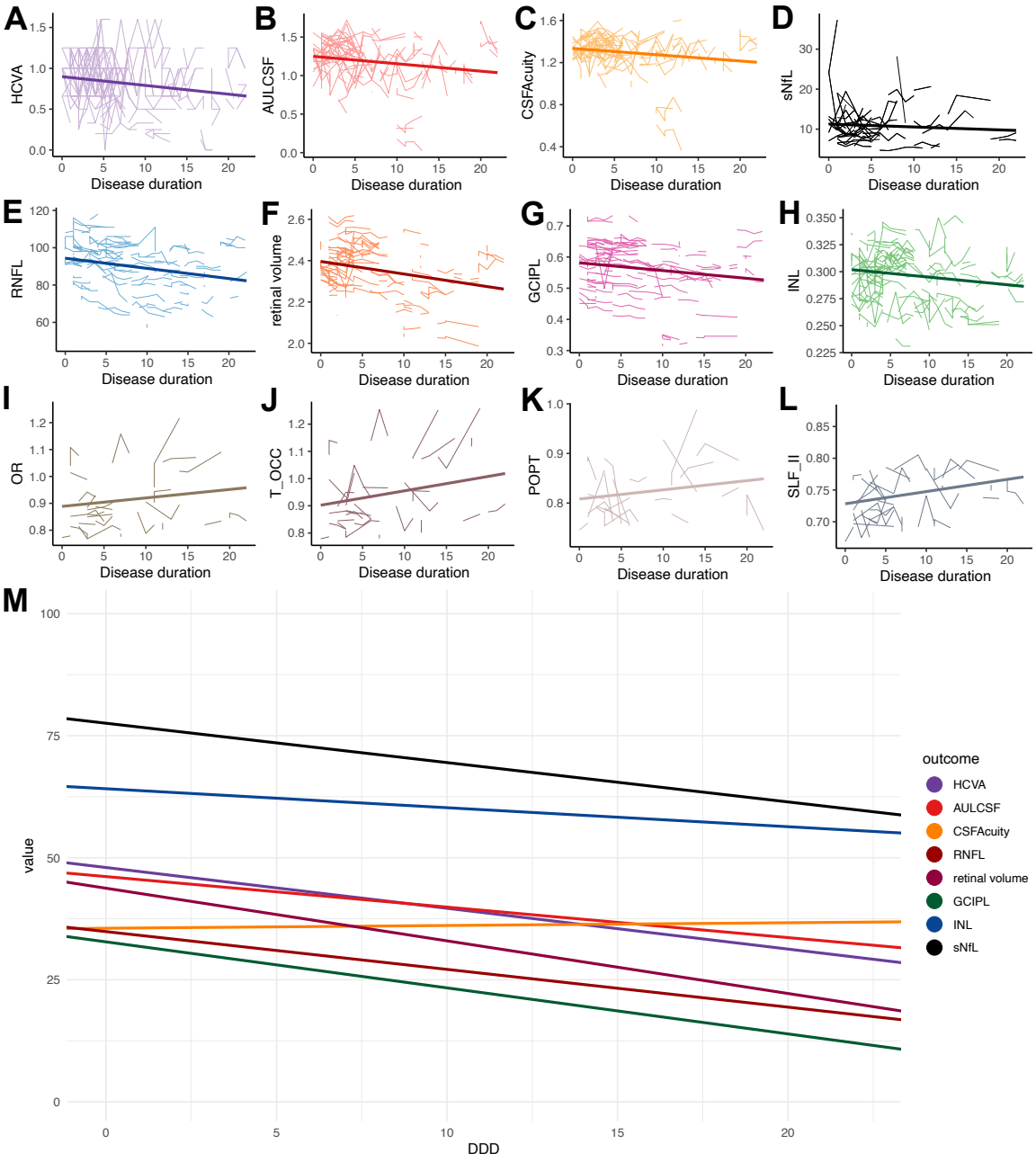

Disease duration and outcomes: Lineplots for each patient or patients' eye with linear regression estimates for visual outcomes (**A-C**), absolute sNfL in pg/ml (**D**), retinal layers (**E-H**) and tracts in the visual system (**I-L**). Mean diffusivity values for tracts are only available for a subset of patients (n = 42). (**M**) Average change in age-adjusted percentile ranks during the disease. Intercepts and slopes estimated with LMER. sNfL percentile ranks are based on the external normative cohort, other

percentile ranks were computed in comparison to the healthy control cohort. Diffusion data could not be included in panel M due to the lack of reference data for percentile rank computation.

Figure 3: Association between structure and function in the visual system

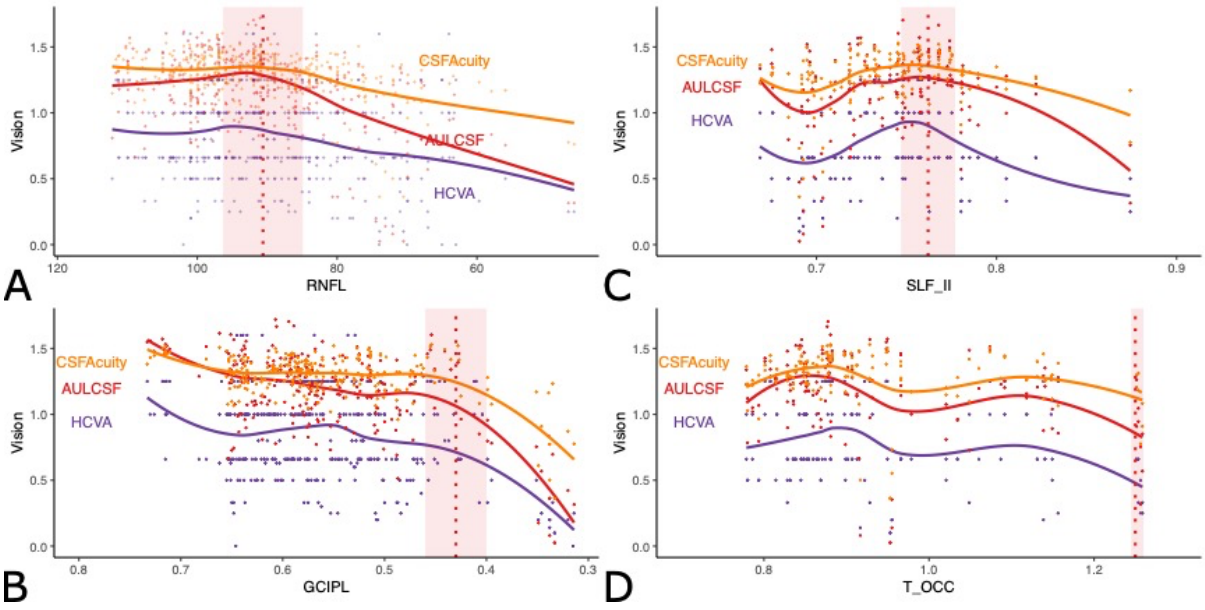

Significant associations between visual functional tests (raw values for HCVA, AULCSF and CSF Acuity on the y-axis), retinal integrity and optic tracts: OCT outcomes on the left panels: (A) RNFL thickness and (B) GCIPL volume. The x-axis is inverted for retinal layers so that the thickness decreases from left to right, i.e., with disease progression. Average mean diffusivity in tracts is displayed on the right panels for (C) SLF II and (D) T_OCC. Dotplots of individual patient data are shown with smooth lines produced from local regression estimates (Loess). Red dotted line indicates the estimated turning point from segmented regression (the shaded area indicates the 95%CI).